Reliable imaging of ATP in living budding and fission yeast

Masak Takaine[1,2]*, Masaru Ueno[3,4], Kenji Kitamura[5], Hiromi Imamura[6], Satoshi Yoshida[1,2,7,8]*

[1]Gunma University Initiative for Advanced Research (GIAR), Gunma University, Maebashi 371-8512, Japan
[2]Institute for Molecular and Cellular Regulation (IMCR), Gunma University, Maebashi 371-8512, Japan
[3]Department of Molecular Biotechnology, Graduate School of Advanced Sciences of Matter, Hiroshima University, Japan
[4]Research Center for the Mathematics on Chromatin Live Dynamics, Hiroshima University, Japan
[5]Center for Gene Science, Hiroshima University, 1-4-2 Kagamiyama, Higashi-Hiroshima 739-8527, Japan
[6]Graduate School of Biostudies, Kyoto University, Kyoto 606-8501, Japan
[7]School of International Liberal Studies, Waseda University, Tokyo, 169-8050, Japan
[8]Japan Science and Technology Agency, PREST

*Correspondence should be addressed to: masaktakaine@gunma-u.ac.jp (M.T.) (Lead contact) or satosh@waseda.jp (S.Y.)

SUMMARY STATEMENT

Budding and fission yeast strains stably expressing an ATP biosensor QUEEN were constructed. They allow reliable observation of ATP dynamics with high spatiotemporal resolution in living eukaryotic cells.

KEYWORDS

ATP, carbon metabolism, homeostasis, yeast, metabolism, meiosis, mitochondria

JCS Advance Online Article. Posted on 11 March 2019

ABSTRACT

Adenosine triphosphate (ATP) is a major metabolite essential for all living organism. However, our understanding of ATP such as heterogeneity in the cell population or dynamicity in a single living cell are very limited. Here, we optimized an ATP-biosensor QUEEN and monitored the dynamics of ATP with good spatial and temporal resolution in living yeasts. We found stable maintenance of ATP concentration in wild type yeasts regardless of carbon sources or cell cycle stages, suggesting that there exists a mechanism to maintain ATP at a specific concentration. We further found that the ATP concentration is not necessarily an indicator of metabolic activity as there is no clear correlation between ATP level and growth rates. During fission yeast meiosis, we found a reduction in the ATP level suggesting that ATP homeostasis is controlled by differentiation. The use of QUEEN in yeasts offers an easy and reliable assay for ATP dynamicity and will answer various unaddressed questions about eukaryotic cellular metabolism.

INTRODUCTION

Adenosine triphosphate (ATP) is a universal energy currency used in all living organism. The half-life of ATP in our body is estimated to be a few seconds (Mortensen et al., 2011) indicating high demand of this energy currency and suggesting that its synthesis and consumption rates are tightly regulated. Because of its importance, molecular mechanism of ATP synthesis by glycolysis and mitochondrial respiration has been rigorously investigated (Berg et al., 2012; Lehninger et al., 2010). However, little is understood how ATP concentration is maintained in each single cell in different conditions because our knowledge on ATP dynamics is largely based on biochemical analysis, which has poor time resolution compared with the rapid turnover rate of ATP. Biochemical analysis also precludes characterization of heterogeneity of ATP concentration in a population or in a tissue.

Recent development of ATP-biosensors enabled us to monitor changes in ATP concentration in each single living cell (Dong and Zhao, 2016). ATeam, the first FRET-based ATP biosensor, has successfully been introduced into mammalian cells and is now widely been used for visualizing ATP dynamics in living cells (Imamura et al., 2009). The second generation ATP biosensor QUEEN (Yaginuma et al., 2014) uses a single green fluorescent protein (FP), instead of cyan FP/yellow FP combination used for ATeam, and has significant advantages especially for the usage in rapidly growing microorganisms such as yeast. First, it has no maturation time lag between two FPs that can produce dysfunctional sensor in rapidly dividing cells such as bacteria and yeasts (see Discussion for details). Second, it is more resistant for degradation than FRET-based sensor ATeam. Third, QUEEN has 1.7 times wider dynamic range compared with ATeam (Yaginuma et al., 2014).

Using QUEEN, it was reported that there exists unexpectedly large variation of ATP concentration within a clonal population of bacteria (Yaginuma et al., 2014). In addition to negative feedback regulation of metabolites concentration (Chubukov et al., 2014), eukaryotic cells harbor energy-sensing mechanisms such as AMP activated protein kinase (AMPK) (Hardie et al., 2016). Thus, it is expected that the ATP concentration is maintained at a specific concentration in eukaryotes.

Yeasts have provided us excellent model systems for studying eukaryotic biology. Especially, central carbon metabolism, including glycolysis and tricarboxylic acid (TCA) cycle, of yeast has been extensively studied or even engineered because it is important for fermentative industry to produce useful metabolites including ethanol (Borodina and Nielsen, 2014; Gibson et al., 2017). Yeast carbon metabolism also provides a tractable model for energy metabolism of cancer cells since they are similar in that they both synthesize ATP mostly through glycolysis even in the presence of oxygen as long as glucose supply is high, which is known as "aerobic fermentation" or the "Warburg effect" of cancer cells (Diaz-Ruiz et al., 2011). In addition to being an important indicator of cell energy, ATP itself is a common regulator of multiple glycolytic enzymes (Larsson et al., 2000; Mensonides et al., 2013). Therefore, elucidation of cellular dynamics of ATP is essential also for deciphering regulation of glycolytic flux, but has remained unaddressed for aforementioned reasons.

Here, we have applied QUEEN in budding and fission yeasts for the first time and found that the ATP level has little variation within a population suggesting that there is a robust ATP homeostasis in eukaryotic cells. We further found that the concentration of ATP is maintained at a constant level regardless of the carbon sources and has no obvious correlation with the mitotic growth phase and growth rates. However, we found that the ATP level declines during fission yeast meiosis suggesting that ATP homeostasis is controlled by developmental context, not by the availability of the sugar.

Taken together, visualization of ATP dynamics in yeast reveals the existence of robust ATP homeostasis. QUEEN-expressing yeasts are useful tools for studying metabolic activity in each individual cell and offers opportunities for testing ATP dynamics in various environmental conditions and in various mutants.

RESULTS

QUEEN is a reliable ATP biosensor in the budding yeast cells

To monitor the dynamics of ATP concentration in each single living cell, we have recently developed several ATP indicators including ATeam (Imamura et al., 2009) and QUEEN (Yaginuma et al., 2014). To explore ATP homeostasis in budding yeast *Saccharomyces cerevisiae*, we chose QUEEN because it has several strongpoints (*see* Introduction). The unique feature of the fluorescent protein QUEEN is that the binding to ATP shifts its optimal excitation wavelength from 480 nm to 410 nm (Fig. 1A), which allows us to estimate the ATP level by quantification of the ratio of the fluorescence signal intensities excited at 410 nm and 480 nm.

We created a budding yeast strain stably expressing QUEEN-2m (K_d of QUEEN-2m with ATP is ~4.5 mM at 25˚C, comparable with estimated cellular ATP concentration in glucose grown yeast) under *TEF1* (translation elongation factor 1α) promoter from the *HIS3* locus. The QUEEN protein was expressed at a similar level in a clonal population and evenly distributed both in the cytoplasm and in the nucleus due to its small size (42 kD) but excluded from the vacuole (Fig. 1B). The QUEEN was sequentially excited by 480 nm and 410 nm lights, and both emitted fluorescence signals at around 520 nm were imaged to calculate the QUEEN ratio (410ex/480ex) of each pixel. The mean of the QUEEN ratios in the intracellular region reflects the ATP concentration of the cell. (*see* Materials and Methods for details).

First, we tested if the QUEEN ratio indeed reflects the cellular concentration of ATP in living yeast. A previous biochemical study demonstrated that ATP levels in budding yeast cells dropped to the 15% upon glucose depletion and is gradually recovered to the 50% of the original level within 20 min (Xu and Bretscher, 2014). Moreover, replacement of glucose in medium with 2-deoxy-D-glucose (2DG), which strongly inhibits glycolysis, reduced the cellular ATP level to less than 1% for a long period of time (Serrano, 1977; Xu and Bretscher, 2014). The QUEEN ratio in yeast cells rapidly dropped after glucose removal (Fig. 1C, 3 min) but partially recovered within 30 min (Fig. 1C). In addition, replacement of glucose with 2% 2DG resulted in rapid and prolonged reduction in the QUEEN ratio (Fig. 1C). Thus, the QUEEN ratio nicely reflects cellular ATP concentration analyzed by biochemical methods.

We also tested if the QUEEN can reversibly monitor the change of ATP concentration. We took advantage of *gph1*Δ mutant cells, which cannot catabolize glycogen, and do not show any recovery of ATP after glucose depletion (Xu and Bretscher, 2014). The mean QUEEN ratios in glucose-depleted *gph1*Δ cells declined rapidly within 10-15 minutes, but re-feeding of glucose fully recovered these values within a minute (Fig. 1D), indicating that the reduction of QUEEN ratio after glucose depletion was not due to an irreversible damage caused to the QUEEN. Taken together, these results suggest that the QUEEN ratio reliably reflects ATP levels in individual cells and allows us to monitor the dynamicity of ATP concentration in living cells. We were also able to estimate the actual ATP concentration in the cell based on the QUEEN ratio by fitting the acquired QUEEN ratio with the calibration curve (Yaginuma et al., 2014) (Fig. S1 and see Materials and Methods for details).

One of the advantages of the use of QUEEN compared with classical biochemical measurements is in its time resolution. We can now monitor the dynamic change of ATP concentration in seconds, which allows us to measure metabolic activity of individual living yeast cells. An example is shown in Fig. 1E, where we monitored the QUEEN ratio after the treatment with 2DG. This analysis suggests that the half-life of ATP in glycolytic condition is less than a minute in budding yeast.

We also have generated QUEEN constructs targeted for mitochondrial matrix (mitQUEEN) and for the surface of endoplasmic reticulum (ER) (erQUEEN) for possible analysis of local ATP concentration (Fig. 1F). In the case for mitochondria, we found that the QUEEN ratio (ATP concentration) in the mitochondria is lower than that in the cytoplasm when grown in a glycolytic condition containing 2% glucose (Fig. S2), similar to what has been reported in HeLa cells using ATeam (Imamura et al., 2009). The detailed use of mitQUEEN and erQUEEN will be described elsewhere and we focus on the ATP in the cytoplasm and nucleus in this report. These results collectively demonstrated that the QUEEN is a useful ATP reporter in budding yeast.

Contribution of carbon sources and respiration to ATP concentration

With the QUEEN system, we are now able to monitor the ATP level in each living cells in various conditions. First, to examine the effect of carbon source utility on ATP, we analyzed QUEEN ratios in cells grown in different hexoses. None of the hexoses tested (2% fructose, 2% galactose, 2% glucose, 2% mannose) significantly affected the ATP concentration (Fig.

2A), suggesting that the ATP level is stably maintained regardless of the carbon sources. We also examined contribution of mitochondrial respiration in ATP levels by treatment with the respiration inhibitor antimycin A (Walther et al., 2010). Antimycin A treatment (2 μg/ml) only slightly reduced (~20%) the ATP levels in cells growing in all the hexoses tested (Fig. 2A), suggesting that the respiration has relatively minor role in ATP synthesis when there is enough carbon source.

Next we explored the effect of fermentative or non-fermentative carbon sources on ATP concentration. Depletion of fermentative carbon source glucose resulted in rapid drop of QUEEN ratio within 3 min, followed by a gradual recovery after 3 hours (Fig. 2B). This recovery was due to activation of respiration because treatment of antimycin A suppressed the QUEEN ratio (Fig. 2B). When cells were grown in non-fermentative carbon glycerol, the ATP level was comparable as to glucose-grown culture, and removal of the glycerol had small effect on the QUEEN ratio even after 3 hours. The high ATP level maintained in glycerol grown cells was due to active respiration as the treatment with antimycin A significantly suppressed it (Fig. 2B). Altogether, our visualization of ATP by QUEEN confirmed that yeast cells growing in fermentative carbon depend heavily on glycolysis to yield cellular ATP (Barnett and Entian, 2005), whereas yeast cells grown in the non-fermentative carbon source are potentiated for respiration (Kayikci and Nielsen, 2015; Shashkova et al., 2015) consistent with the observation that glycerol-grown yeast has highly developed mitochondria (Egner et al., 2002).

ATP concentration during budding yeast cell cycle

Next, we also analyzed ATP concentration during mitotic cell cycle. The QUEEN ratio was followed over generations by time-lapse imaging using Myo1-mCherry as a bud neck marker indicative of budded stages. In a clear contrast to what has been observed in bacteria (Yaginuma et al., 2014), there was little fluctuation of ATP level in rapidly growing yeast in 2% glucose (Fig. 3A, B; movie S1). We also quantified the QUEEN ratio in the cells at different cell cycle stages such as unbudded (G1), small budded (S) or large budded (G2 and M), but did not find significant difference in each cell cycle stages (Fig. 3C). Little fluctuation of ATP concentrations during the cell cycle in each single cell and among the population suggest that there exists a mechanism for stably maintaining ATP concentration in yeast. Stable maintenance of ATP during the cell cycle was also observed in the cells cultured in glycerol (Fig. 3D), suggesting that neither glycolysis nor respiration is significantly regulated during the cell cycle.

QUEEN is a reliable ATP biosensor in the fission yeast

Next we examined the use of QUEEN in fission yeast *Schizosaccharomyces pombe*. QUEEN construct was integrated to the *leu1* locus of the chromosome and expressed under *TEF51* (translation elongation and termination factor eIF5A) promoter. QUEEN protein was evenly distributed both in the cytoplasm and in the nucleus (Fig. 4A). The QUEEN ratio was calculated in the same manner as in *S. cerevisiae*, and we found that relatively high QUEEN ratio in fission yeast cells grown in EMM medium containing 2% glucose, but the ratio dropped within 5 minutes after replacing the medium containing 20 mM 2DG and 10 μg/ml antimycin A (Fig. 4A, B). This suggests that the QUEEN ratio is reflecting the intracellular concentration of ATP in fission yeast. We also note that the half-life of ATP in glycolytic condition is about 1-2 minutes in fission yeast, as judged by a rapid reduction in QUEEN ratio after 2DG treatment (Fig. 4C).

Contribution of glycolysis and respiration on fission yeast ATP

It is known that growth of fission yeast largely rely on glycolysis when there are high concentration of glucose, but rely on respiration for survival when glucose is limited (Takeda et al., 2015) . To examine the relative contribution of glycolysis and respiration in the ATP level, we monitored the QUEEN ratio of fission yeast grown in different glucose concentration. In the presence of 2% or 0.02% glucose, cells contain about 3 mM ATP. Even after 6 hours of glucose depletion, cells are viable and maintained 2.3 mM ATP (Fig. 5A, B). The contribution of glucose and mitochondria on ATP level was clearly counter-correlated. Treatment of antimycin A had a minor effect on the ATP level in the cells grown in the 2% glucose, but had a larger effect in the cells grown in the 0.02% glucose cells (Fig. 5A, B). Respiration was essential for ATP production in the absence of glucose. Glucose-depleted cells completely lost cellular ATP after the treatment with antimycin A for 10 minutes (Fig. 5A, B).

Our analysis of ATP concentration is in a good accordance of recent study by Takeda et al. that glucose has dominant role in cellular energestics and respiration play major role when glucose concentration is severely limited (Takeda et al., 2015). Thus, QUEEN is a reliable and useful indicator of ATP concentration in fission yeast.

ATP concentration during fission yeast mitotic cell cycle

We examined if ATP concentration fluctuates during the fission yeast cell cycle. The unique feature of fission yeast is that the cell cycle stage is tightly correlated with its length (Mitchison and Nurse, 1985). We quantified the QUEEN ratio in the cells with various length but did not find significant relationship between the QUEEN ratio and the cell length, suggesting that ATP concentration does not change during mitotic cell cycle (Fig. 6A). Time-lapsed imaging of the QUEEN ratio of mitotically growing cells further confirmed that ATP level has little fluctuation during a cell cycle in fission yeast in 2% glucose (Fig. 6B, C and movie S2).

ATP concentration during fission yeast sporulation

We also examined the QUEEN ratio in sporulating fission yeast. Fission yeast undergoes meiotic cell cycle when nitrogen source is depleted. We first confirmed that depletion of nitrogen (in the presence of 2% glucose) did not affect cellular ATP level for the first 30 min (Fig. 7A, C). After 16-hour removal of nitrogen, there were a mixed population of fission yeast cells undergoing various stages of meiosis (Yamashita et al., 2017). We found a partial decline in the QUEEN ratio in cells undergoing meiosis (Fig. 7A, B). Treatment with antimycin A (for 30 min) or 2DG (for 10 min) revealed that the glycolysis is the major source of ATP during meiosis (Fig. 7A). After sporulation, we found that the ATP level was further declined in the remnant cytoplasm but was maintained at higher level inside the spores (Fig. 7B, D). The ATP level in the spore seemed to be also due to glycolysis but not due to mitochondria as treatment with 2DG but not antimycin for 2 hours had a significant effect (Fig. 7B). These results reveal that ATP level is controlled both temporally and spatially during meiosis and glycolysis plays pivotal role in the ATP synthesis during meiosis.

Discussion

In this study, we visualized ATP dynamics in both budding and fission yeasts using ATP biosensor QUEEN for the first time in eukaryotic cells. In a clear contrast with bacterial cells, there is little fluctuation/variation in the ATP concentration in yeast population in the same culture. Furthermore, we found that the ATP concentration in yeast is remarkably constant regardless of the carbon sources or of the cell cycle stages suggesting a robust ATP homeostasis in eukaryotic cells.

We have shown that the QUEEN has a wide dynamic range optimal for physiological concentration of ATP in yeast cells and have established a reliable and sensitive assay for ATP concentration in living yeasts The QUEEN expressing yeast strains and plasmids are publically available from the Yeast Genetic Resource Centre Japan (YGRC, http://yeast.nig.ac.jp/yeast/top.xhtml). Visualization of ATP by QUEEN offers many advantages that were impossible or very difficult to examine by standard biochemical assays. These include but are not limited to the followings:

1. The reversibility of QUEEN signal allows us to monitor the dynamics of ATP concentration in a single living cell.
2. We have much higher time resolution compared with standard biochemical assays.
3. We may be able to monitor subcellular distribution of ATP using organelle-targeted QUEEN.
4. We can observe variation in the ATP concentration in a life of a single cell or in a lineage and among the population.

There have been several attempts to visualize ATP in living yeasts. One approach using DNA aptamer for ATP made a success in real time visualization of budding yeast ATP (Ozalp et al., 2010). However, the use of the aptamer is limited because introduction of the aptamer to the cells is an invasive and hard-to-control step. FRET-based ATP biosensor ATeam is widely used in mammalian system, but is not suitable for rapidly proliferating yeasts (doubling time of 90–100 min) because long maturation time of the sensor and the presence of malfunctioning sensors would lead to unreliable outcomes as observed in using of ATeam in growing bacteria (Yaginuma et al., 2014). Thus, we believe that QUEEN is the best ATP biosensor for yeasts currently available.

Using QUEEN, we found that ATP is maintained at a stable concentration (3–4 mM) regardless of the growth conditions suggesting that there exists a mechanism to maintain ATP concentration at a certain level. We also note that the mean ATP concentration in budding yeast cells in 2% glucose calculated from the QUEEN ratio (3.2 ± 0.4 mM, Fig. 2) shows good agreement with intracellular ATP concentrations estimated by biochemical analysis (4 mM or 4.6 mM (Gauthier et al., 2008; Ljungdahl and Daignan-Fornier, 2012)), demonstrating reliability of QUEEN and the validity of our calibration method. Using QUEEN, we have previously reported that there is a large variation in the cellular ATP level in rapidly proliferating bacteria. In contrast to bacteria, we found little variation in the cellular concentration of ATP in yeast regardless of the growth conditions suggesting that there exists a mechanism to maintain ATP concentration in eukaryotic cells.

It has been proposed that concentrations of the metabolites are generally regulated by negative feedbacks (Chubukov et al., 2014). Excessive ATP can inhibit glycolysis by allosterically inactivating phosphofructokinases and pyruvate kinases (Larsson et al., 2000; Reibstein et al., 1986). In eukaryotic cells, reduction of ATP (and increase of AMP) activates AMP activated protein kinase (AMPK) and AMPK, in turn, is thought to suppress ATP consumption (Hardie et al., 2016). It will be of interest to define the detailed molecular mechanisms which lead to stable maintenance of ATP in yeast.

Because ATP is essential for many cellular functions, ATP concentration is often used as an indicator of cellular activity. It is surprising to find that the cellular concentration of ATP is similar in the cells grown in the presence or absence of glucose because both budding and fission yeasts proliferate significantly slower in the absence of carbon sources (Takeda et al., 2015; Tyson et al., 1979). Our study also revealed that the ATP concentration is stably maintained during normal cell cycle in both yeasts. It is anticipated that the cellular energy consumption rate is under the cell cycle control because the rate of cell growth is affected by the cell cycle (Goranov et al., 2009) and there are various energy consuming events such as DNA replication in S-phase or chromosome segregation in mitosis. Our findings suggest that there exists a mechanism to maintain ATP concentration at a certain level regardless of the growth speed or cell cycle stages. Thus, ATP concentration is unlikely a direct indicator of the metabolic activity and we need to monitor the turnover-rate of ATP for measuring cell activity. The use of QUEEN offers an easy and reliable assay for ATP turnover-rate compared with standard biochemical assays.

The QUEEN expressing yeast enabled us to monitor the ATP level during fission yeast meiosis for the first time. The ATP level partially declines when cells enter meiosis and the ATP level was maintained relatively high only inside the spores. The mechanism by which ATP in the spore but not in the cytoplasm was maintained requires further investigation. In addition, the ineffectiveness of antimycin A against ATP level in spores does not rule out the possibility that mitochondrial respiration also contributes to maintain ATP in spores because the drug might be hardly permeable to spore membrane. The requirement of glycolysis but not respiration for ATP synthesis during fission yeast meiosis is somewhat confusing because fission yeast defective in respiration fails in sporulation (Jambhekar and Amon, 2008). This suggest that the requirement of mitochondria in sporulation may involve steps other than ATP synthesis such as lipid and amino acids metabolism. Alternatively, respiration may play more dominant role in fission yeast meiosis in a natural condition where carbon source may be also limited (2% glucose was added in our sporulation assay).

Mechanism of the decrease in meiotic ATP level is also unknown, but our analysis suggests that the change in glycolytic activity, not respiration is contributing it. It has been reported that the expression level of metabolic enzymes including glycolytic enzymes are largely altered during meiosis in fission yeast (Mata et al., 2002; Yamamoto, 1996) suggesting that the metabolic activity and ATP homeostasis is remodeled during this differentiation process.

Live cell imaging of metabolites is a powerful approach to discover sporadic events happening in a fraction of the cells in a population or fluctuation within a single cell. The biosensors can also be targeted to the organelle or specific subcellular compartments, allowing the measurement of local concentration of the metabolites (Imamura et al., 2009). Further studies are needed to clarify the metabolic control of fission yeast meiosis, but the use and application of the QUEEN in yeasts is limitless. We are now able to monitor the dynamics of ATP with good spatial and temporal resolution in living yeasts and can explore various unaddressed questions about ATP level such as during diauxic shift, starvation, stress response, differentiation and aging. Furthermore, the easy measurements of ATP consumption rate by QUEEN system allow us to analyze metabolic activity in single cell in various conditions. The use of QUEEN in yeasts may bring our understanding of bioenergetics to another level.

MATERIALS AND METHODS

Yeast strains and plasmids

Budding and fission yeast strains, and plasmids used in this study are listed in the Tables S1, S2, and S3, respectively. These strains were constructed by a PCR-based method (Janke et al., 2004) and genetic crosses. The yeast knockout strain collection was originally purchased from GE Healthcare (cat# YSC1053). Some plasmids were originally purchased from EUROSCARF (Oberursel, Germany). Construction of the fission yeast strain expressing QUEEN (KSP3769) is described elsewhere (Ito et al., 2019, accepted).

The QUEEN-expressing budding yeast strains were constructed as follows. First, the QUEEN-2m ORF was isolated by cutting pRSETb-QUEEN-2m (Yaginuma et al., 2014) with *BamH*I and *Hind*III, and ligated into *BamH*I/*Hind*III sites of pSP-G2 (Partow et al., 2010) to yield MTP3051. Next, a *Sac*I/*BamH*I fragment of *S. cerevisiae TEF1* (translation elongation factor 1α) promoter from pYM-N19 (Janke et al., 2004; Mumberg et al., 1995) and a *BamH*I/*Pvu*II fragment of the QUEEN-2m ORF flanked with *CYC1* terminator from MTP3051 were inserted by trimeric ligation into the *Sac*I-*EcoR*V sites of pRS303 to yield MTP3067. For expression of QUEEN-2m from the *his3* locus, MTP3067 was linearized by *Pst*I and integrated into the *his3*Δ*1* locus of the wild-type strain MTY3015 to yield MTY3255 and 3261. Integrations and the copy number of the QUEEN were confirmed by diagnostic PCR and western blotting.

A budding yeast strain expressing a QUEEN construct that localizes to mitochondrial matrix was generated as follows. First, a DNA fragment encoding a two tandem copies of mitochondrial targeting signal sequence of human cytochrome *c* oxidase subunit VIII and the first 20 amino acid sequence of QUEEN-2m was artificially synthesized with codon optimization for yeasts (Eurofin Genomics, Ebersberg, Germany). Next, the DNA fragment was inserted into the *Xba*I-*EcoR*V sites of MTP3067 to yield MTP3079. MTP3079 was linearized and integrated into the *his3*Δ*1* locus of MTY3015 to yield MTY3227.

A budding yeast strain expressing a QUEEN construct that localizes to the cytoplasmic surface of endoplasmic reticulum was generated as follows. First, a DNA fragment encoding the SEC71TMD (Sato et al., 2003) and its neighboring sequences (40 amino acids), a five-glycine linker and the first 20 amino acid sequence of QUEEN-2m was artificially synthesized (Eurofin Genomics). Next, the DNA fragment was inserted into the *Xba*I-*EcoR*V sites of MTP3067 to yield MTP3080. MTP3080 was linearized and integrated into the *his3*Δ*1* locus of MTY3015 to yield MTY3229.

All new strains and plasmids would be deposited to and be available from the Yeast Genetic Resource Centre Japan (YGRC, http://yeast.nig.ac.jp/yeast/top.xhtml).

Media, cell culture

Synthetic medium (SC) for budding yeast was prepared according to the recipe of Hanscho et al. (Hanscho et al., 2012). Complete (YE), synthetic (EMM) and malt extract (ME) media for fission yeast were prepared according to the recipe of Forsburg et al. (Forsburg and Rhind, 2006). YE and EMM media were supplemented with 100 µg/ml adenine, 20 µg/ml uracil, 20 µg/ml L-histidine, 30 µg/ml L-lysine and 60 µg/ml L-leucine. Cells were grown to mid-log at 30°C in synthetic media before imaging unless otherwise noted. 2-deoxy-D-glucose (2DG) was purchased from FUJIFILM Wako (Osaka, Japan) (cat# 046-06483) and dissolved in media instead of glucose. Antimycin A was purchased from FUJIFILM Wako (cat# 514-55521) and dissolved in dimethylsulfoxide (DMSO) to make a stock solution (20 mg/ml).

To induce mating and meiosis of fission yeast cells, homothallic MTY1162 cells were grown to mid-log in liquid YE, washed with water two times, and then incubated on an ME plate for 14–20 h at 25°C. Zygotes and asci in the culture were suspended in EMM lacking a nitrogen source (EMM−N) and subjected to microscopy.

Microscopy

Budding and fission yeast cells were immobilized on a 35-mm-glass bottom dish (#3971-035, No. 1.5 thickness, IWAKI, Shizuoka, Japan) coated by concanavalin A (C-7275, Sigma-Aldrich, St. Louis, US) or soybean lectin (L-1395, Sigma-Aldrich), respectively, unless otherwise noted. The dish was filled with excess amount of medium (4.5–5 ml) against the cell volume to minimize changes in chemical compositions of the medium during observation. In some cases (Figs. 1B-D, 1F, 3C), cells were concentrated by centrifugation and sandwiched between a slide and a coverslip (No. 1.5 thickness, Matsunami, Osaka, Japan). In the latter case, imaging was completed within a few minutes after the preparation. The immobilized cells were imaged using an inverted fluorescent microscope (Eclipse Ti-E, Nikon, Tokyo, Japan) equipped with Apo TIRF 100x Oil DIC N2/NA 1.49 objective lens and an electron multiplying charge-coupled device camera (iXon3 DU897E-CS0-#BV80, Andor-Oxford Instruments, Abingdon, UK) at around 25°C. The QUEEN fluorescence emitted around 520 nm upon excitation at 480 nm and at 410 nm was collected from a single *z*-plane using a FITC filter set (Ex465-495/DM505/BA515-555, Nikon) and a custom-made filter set (Ex393-425/DM506/BA516-556, Semrock, New York, US), respectively. We sometimes

imaged the QUEEN fluorescence signals using an FV-1000 confocal laser scanning microscope (Olympus, Tokyo, Japan) (Figs. 1B-D, 2B, 3C) equipped with UPLSAPO 100xO/NA 1.4 objective lens (Olympus) with excitation by 473-nm and 405-nm lasers using a dichroic mirror DM405/473 and a barrier filter BA490-540. The QUEEN fluorescent signal from mitochondrial matrix was collected from stacks of 11 *z*-sections spaced by 0.5 μm. Images of cells were acquired from several fields of view for each experimental condition, giving enough sample size for quantitative analysis.

Data analysis and calculation of QUEEN ratio

Acquired digital images were analyzed using a Fiji software (Schindelin et al., 2012). The fluorescence images of QUEEN upon excitation at around 480 nm (ex480 image) or around 410 nm (ex410 image) were collected as described above. The QUEEN ratio was calculated as follows. First, the both QUEEN images were converted to signed 32-bit floating-point grayscale and then corrected for background using the rolling-ball algorithm or by subtracting the mean pixel values in an area outside the cells. Next, the images were thresholded using the modified IsoData algorithm to set background (non-thresholded) pixels to the *NaN* (Not a Number) value. The ex410 image was divided by the ex480 image to calculate the QUEEN ratio at each pixel. The ratio images were expressed in pseudocolor with appropriate lookup-tables and display range. The mean ratio in pixels corresponding the inside of a cell was used to represent the ATP level of the cell.

Cell boundaries in the ratio image were determined as follows. The QUEEN images were merged, and then thresholded to generate a binary image. Particles (corresponding to cells expressing QUEEN) in the binary image were analyzed and automatically outlined to draw regions of interest (ROIs) of the cells. Alternatively, ROIs of cells were manually drawn. Numerical data were plotted using a KaleidaGraph software ver. 4.5.1 (Synergy Software, PA, US) or the R studio software ver. 3.4.1 (R Core Team, 2017).

Estimation of ATP concentration from the QUEEN ratio in yeast

Based on the biochemical data (Serrano, 1977; Xu and Bretscher, 2014), we assumed that the ATP is depleted when cells were treated with 2DG in budding yeast. We quantified the QUEEN ratio in the cells treated with 2DG in the absence of glucose with our Eclipse Ti-E, Nikon microscope system (Fig. S1A, B) and adjusted the calibration curve previously published (Yaginuma et al., 2014) with the zero-point. This calibration curve was used for the

estimation of ATP concentration in yeast cells when the QUEEN ratio was analyzed with the Nikon system.

The QUEEN ratio in the budding yeast cells in 2% glucose medium was about 2.7-fold higher than that in the cells treated with 2DG. Therefore, the dynamic range of the QUEEN ratio is at least 2.7 under our experimental conditions. This is in good agreement with the previous result showing the dynamic range of QUEEN in bacteria is at least 3.0-fold (Yaginuma et al., 2014).

Statistical analysis

Means, SDs, and *p*-values were calculated using Excel software (Microsoft, WA, US). Significance between two sets of data was tested using an unpaired one-tailed Welch's *t*-test and was indicated by an asterisk. The horizontal bar in dot plot indicates the average of each population. We plotted and compared data obtained from experiments done on the same day and did not pool data from experiments done on different days because several factors vary slightly day-to-day and can affect QUEEN ratio: for example, room temperature, batch of medium, intensity of excitation light, conditions of optical filters for fluorescence microscopy and cell density. All the measurements of QUEEN ratio were repeated at least twice.

ACKNOWLEDGMENTS

We thank members of Yoshida/Takaine labs for their support. We also thank K. Ohashi, R. Chaleckis and F. Matsuda for valuable discussion and comments, and the Yeast Genetic Resource Center (Osaka City University, Japan) for providing plasmids.

AUTHOR CONTRIBUTIONS

Conceptualization: M.T., S.Y.; Methodology: M.T.; Validation: M.T., M.U., K.K; Formal analysis: M.T.; Investigation: M.T., M.U., S.Y.; Resources: M.T., K.K., H.I.; Data curation: M.T., M.U.; Writing - original draft: M.T., S.Y.; Writing - review & editing: M. T., M.U., K.K., H.I., S.Y.; Supervision: M.T., S.Y.; Funding acquisition: M.T., M.U., S.Y.

COMPETING INTERESTS

The authors declare no competing interests.

FUNDING

This work was supported by JSPS grants 16H04781 (S.Y. and M.T.), 15K18525 (M.T.) and Takeda Science foundation (S.Y.). This work was also supported by a joint research program of the Institute for Molecular and Cellular Regulation, Gunma University, Japan (M.U. and M.T.).

REFERENCES

Barnett, J. A. and Entian, K. D. (2005). A history of research on yeasts 9: regulation of sugar metabolism. *Yeast* **22**, 835-94.

Berg, J., Tymoczko, J. and Stryer, L. (2012). Biochemistry VIIth edition: WH Freeman and Company, New York.

Borodina, I. and Nielsen, J. (2014). Advances in metabolic engineering of yeast Saccharomyces cerevisiae for production of chemicals. *Biotechnol J* **9**, 609-20.

Chubukov, V., Gerosa, L., Kochanowski, K. and Sauer, U. (2014). Coordination of microbial metabolism. *Nat Rev Microbiol* **12**, 327-40.

Diaz-Ruiz, R., Rigoulet, M. and Devin, A. (2011). The Warburg and Crabtree effects: On the origin of cancer cell energy metabolism and of yeast glucose repression. *Biochim Biophys Acta* **1807**, 568-76.

Dong, J. and Zhao, M. (2016). In-vivo fluorescence imaging of adenosine 5′ -triphosphate. *TrAC Trends in Analytical Chemistry* **80**, 190-203.

Egner, J., S, H. and SW. (2002). Fast 100-nm resolution three-dimensional microscope reveals structural plasticity of mitochondria in live yeast. *Proc Natl Acad Sci U S A* **99**, 3370-5.

Forsburg, S. L. and Rhind, N. (2006). Basic methods for fission yeast. *Yeast* **23**, 173-83.

Gauthier, S., Coulpier, F., Jourdren, L., Merle, M., Beck, S., Konrad, M., Daignan-Fornier, B. and Pinson, B. (2008). Co-regulation of yeast purine and phosphate pathways in response to adenylic nucleotide variations. *Mol Microbiol* **68**, 1583-94.

Gibson, B., Geertman, J. M. A., Hittinger, C. T., Krogerus, K., Libkind, D., Louis, E. J., Magalhães, F. and Sampaio, J. P. (2017). New yeasts–new brews: modern approaches to brewing yeast design and development. *FEMS Yeast Research* **17**, fox038-fox038.

Goranov, A. I., Cook, M., Ricicova, M., Ben-Ari, G., Gonzalez, C., Hansen, C., Tyers, M. and Amon, A. (2009). The rate of cell growth is governed by cell cycle stage. *Genes Dev* **23**, 1408-22.

Hanscho, M., Ruckerbauer, D. E., Chauhan, N., Hofbauer, H. F., Krahulec, S., Nidetzky, B., Kohlwein, S. D., Zanghellini, J. and Natter, K. (2012). Nutritional requirements of the BY series of Saccharomyces cerevisiae strains for optimum growth. *FEMS Yeast Res* **12**, 796-808.

Hardie, D. G., Schaffer, B. E. and Brunet, A. (2016). AMPK: An Energy-Sensing Pathway with Multiple Inputs and Outputs. *Trends Cell Biol* **26**, 190-201.

Imamura, H., Nhat, K. P., Togawa, H., Saito, K., Iino, R., Kato-Yamada, Y., Nagai, T. and Noji, H. (2009). Visualization of ATP levels inside single living cells with fluorescence resonance energy transfer-based genetically encoded indicators. *Proc Natl Acad Sci U S A* **106**, 15651-6.

Jambhekar, A. and Amon, A. (2008). Control of Meiosis by Respiration. *Current Biology* **18**, 969-975.

Janke, C., Magiera, M. M., Rathfelder, N., Taxis, C., Reber, S., Maekawa, H., Moreno-Borchart, A., Doenges, G., Schwob, E., Schiebel, E. et al. (2004). A versatile toolbox for PCR-based tagging of yeast genes: new fluorescent proteins, more markers and promoter substitution cassettes. *Yeast* **21**, 947-62.

Kayikci, O. and Nielsen, J. (2015). Glucose repression in Saccharomyces cerevisiae. *FEMS Yeast Res* **15**.

Larsson, C., Pahlman, I. L. and Gustafsson, L. (2000). The importance of ATP as a regulator of glycolytic flux in Saccharomyces cerevisiae. *Yeast* **16**, 797-809.

Lehninger, A., Nelson, D. and Cox, M. (2010). Principles of Biochemistry. CBS publisher and distributors: Delhi.

Ljungdahl, P. O. and Daignan-Fornier, B. (2012). Regulation of amino acid, nucleotide, and phosphate metabolism in Saccharomyces cerevisiae. *Genetics* **190**, 885-929.

Mata, J., Lyne, R., Burns, G. and Bähler, J. (2002). The transcriptional program of meiosis and sporulation in fission yeast. *Nat Genet* **32**, 143-7.

Mensonides, F. I., Bakker, B. M., Cremazy, F., Messiha, H. L., Mendes, P., Boogerd, F. C. and Westerhoff, H. V. (2013). A new regulatory principle for in vivo biochemistry: pleiotropic low affinity regulation by the adenine nucleotides--illustrated for the glycolytic enzymes of Saccharomyces cerevisiae. *FEBS Lett* **587**, 2860-7.

Mitchison, J. and Nurse, P. (1985). Growth in cell length in the fission yeast Schizosaccharomyces pombe. *J Cell Sci* **75**, 357-76.

Mortensen, S. P., Thaning, P., Nyberg, M., Saltin, B. and Hellsten, Y. (2011). Local release of ATP into the arterial inflow and venous drainage of human skeletal muscle: insight from ATP determination with the intravascular microdialysis technique. *The Journal of Physiology* **589**, 1847-1857.

Mumberg, D., Muller, R. and Funk, M. (1995). Yeast vectors for the controlled expression of heterologous proteins in different genetic backgrounds. *Gene* **156**, 119-22.

Ozalp, V. C., Pedersen, T. R., Nielsen, L. J. and Olsen, L. F. (2010). Time-resolved measurements of intracellular ATP in the yeast Saccharomyces cerevisiae using a new type of nanobiosensor. *J Biol Chem* **285**, 37579-88.

Partow, S., Siewers, V., Bjorn, S., Nielsen, J. and Maury, J. (2010). Characterization of different promoters for designing a new expression vector in Saccharomyces cerevisiae. *Yeast* **27**, 955-64.

R Core Team. (2017). R: A Language and Environment for Statistical Computing. Vienna, Austria: R Foundation for Statistical Computing.

Reibstein, D., den Hollander, J. A., Pilkis, S. J. and Shulman, R. G. (1986). Studies on the regulation of yeast phosphofructo-1-kinase: its role in aerobic and anaerobic glycolysis. *Biochemistry* **25**, 219-27.

Sato, K., Sato, M. and Nakano, A. (2003). Rer1p, a retrieval receptor for ER membrane proteins, recognizes transmembrane domains in multiple modes. *Mol Biol Cell* **14**, 3605-16.

Schindelin, J., Arganda-Carreras, I., Frise, E., Kaynig, V., Longair, M., Pietzsch, T., Preibisch, S., Rueden, C., Saalfeld, S., Schmid, B. et al. (2012). Fiji: an open-source platform for biological-image analysis. *Nat Methods* **9**, 676-82.

Serrano, R. (1977). Energy Requirements for Maltose Transport in Yeast. *European Journal of Biochemistry* **80**, 97-102.

Shashkova, S., Welkenhuysen, N. and Hohmann, S. (2015). Molecular communication: crosstalk between the Snf1 and other signaling pathways. *FEMS Yeast Res* **15**, fov026.

Takeda, K., Starzynski, C., Mori, A. and Yanagida, M. (2015). The critical glucose concentration for respiration-independent proliferation of fission yeast, Schizosaccharomyces pombe. *Mitochondrion* **22**, 91-95.

Tyson, C. B., Lord, P. G. and Wheals, A. E. (1979). Dependency of size of Saccharomyces cerevisiae cells on growth rate. *J Bacteriol* **138**, 92-8.

Walther, T., Novo, M., Rossger, K., Letisse, F., Loret, M. O., Portais, J. C. and Francois, J. M. (2010). Control of ATP homeostasis during the respiro-fermentative transition in yeast. *Mol Syst Biol* **6**, 344.

Xu, L. and Bretscher, A. (2014). Rapid glucose depletion immobilizes active myosin V on stabilized actin cables. *Curr Biol* **24**, 2471-9.

Yaginuma, H., Kawai, S., Tabata, K. V., Tomiyama, K., Kakizuka, A., Komatsuzaki, T., Noji, H. and Imamura, H. (2014). Diversity in ATP concentrations in a single bacterial cell population revealed by quantitative single-cell imaging. *Sci Rep* **4**, 6522.

Yamamoto, M. (1996). The molecular control mechanisms of meiosis in fission yeast. *Trends Biochem Sci* **21**, 18-22.

Yamashita, A., Sakuno, T., Watanabe, Y. and Yamamoto, M. (2017). Analysis of Schizosaccharomyces pombe Meiosis. *Cold Spring Harb Protoc* **2017**, pdb top079855.

Figures

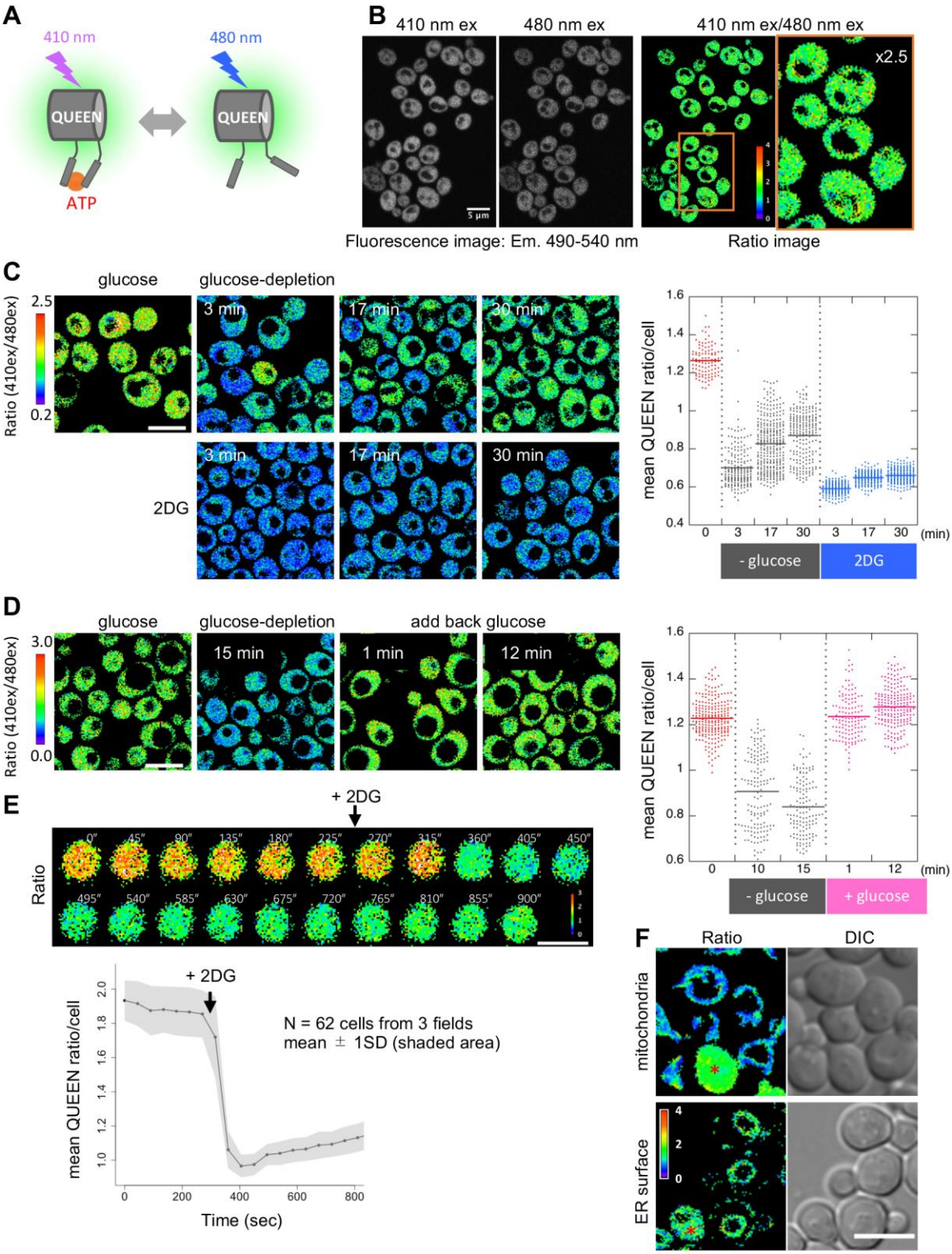

Fig. 1. QUEEN is a reliable ATP biosensor in the budding yeast cells

(A) Design of QUEEN. ATP-bound QUEEN is more readily excited at the 410 nm light while ATP-free QUEEN prefers 480 nm. (B) Fluorescence images of the yeast cells expressing QUEEN. The green fluorescence signal was imaged by excitation at 410 nm or at 480 nm. The QUEEN ratio (410 nm ex/480 nm ex) was calculated from the signal intensity of each pixel to generate the QUEEN ratio image of cells. The QUEEN ratio is pseudo-colored to reflect its value throughout the paper. Insets show 2.5-times magnified images of the boxed region. (C) Time course analysis of the QUEEN ratio after glucose depletion. MTY3255 cells grown in SC medium containing 2% glucose were washed and released either in the medium lacking glucose (top) or in the medium containing 2% 2-deoxy-D-glucose (2DG: bottom). The QUEEN signal excited at the 410 nm and 480 nm light was imaged at the indicated time points. Representative QUEEN ratio images are shown in the left and the mean QUEEN ratios inside the cell were plotted in the right. The horizontal bar indicates an average. N = 101–307 cells were scored. (D) QUEEN can report not only reduction but also recovery of ATP concentration. MTY3153 cells grown in the 2% glucose were released in the medium lacking glucose. After 15 minutes, 2% glucose was added back to the media and the QUEEN signal was imaged at the indicated time points. Left: representative images; right: the dot plot of the mean QUEEN ratio in the cells. N = 137–225 cells were scored. (E) Rapid decrease in QUEEN ratio in cells treated with glycolytic inhibitor. The QUEEN ratio in MTY3264 cells grown in the 2% glucose was sequentially monitored, and the cells were supplemented with 2DG just after t = 270 s (indicated by an arrow) to give a final concentration of 22 mM glucose and 96 mM 2DG. The representative time-lapse image was shown (top). The QUEEN ratio at each time point was plotted (bottom). Data are the mean ± SD (shaded area), and collected from three fields of view. (F) Examples of organelle-localized QUEEN. Mitochondrially targeted QUEEN (top) and ER targeted QUEEN (bottom). For comparison, a cell expressing QUEEN in the cytoplasm was included (asterisk in each panel). White scale bar = 5 μm.

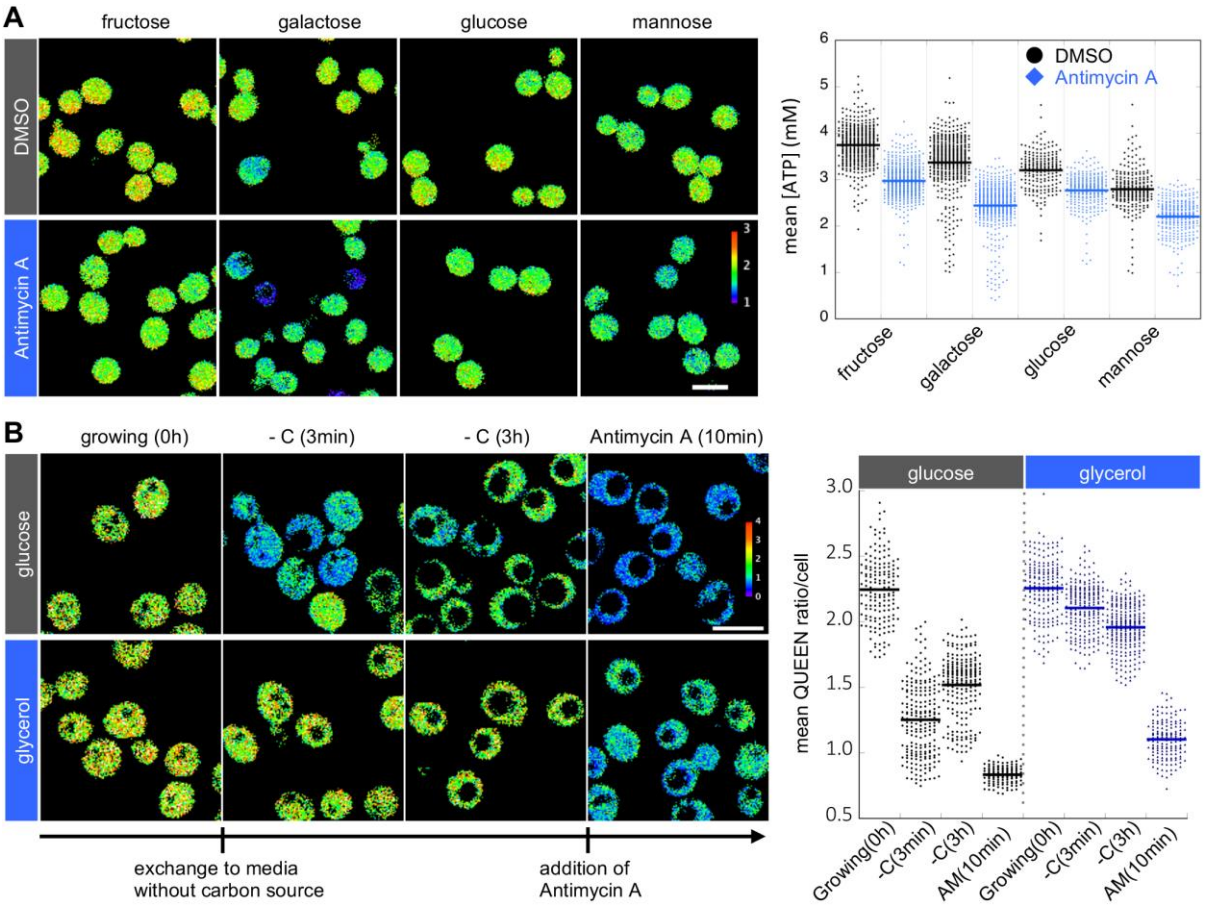

Fig. 2. Budding yeast ATP homeostasis in different growth conditions

(A) ATP concentration in the cells grown in different hexoses (2%). Mean QUEEN ratio of the yeast cells grown in the SC medium containing indicated hexoses as a sole carbon source. The QUEEN images were taken after treatment with 0.05% DMSO (black/top) or 10 µg/ml Antimycin A (blue/bottom) for 30 min. The QUEEN ratio was translated to the ATP concentration (mM), and plotted in the right. N = 198–555 cells were scored. (B) Respiration is the major source of ATP in the absence of fermentative sugar glucose. MTY3255 was grown either in SC + 2% glucose (glucose) or in the SC +3% glycerol +0.1% glucose (glycerol). The cells were washed and released in the SC medium lacking any carbon sources. After 3 hours, the medium was switched with SC (no carbon) with 10 µg/ml Antimycin A (AM). At the indicated time points, QUEEN signals were imaged and the QUEEN ratio of each cell was plotted in the right. N = 126–241 cells were scored. White scale bar = 5 µm.

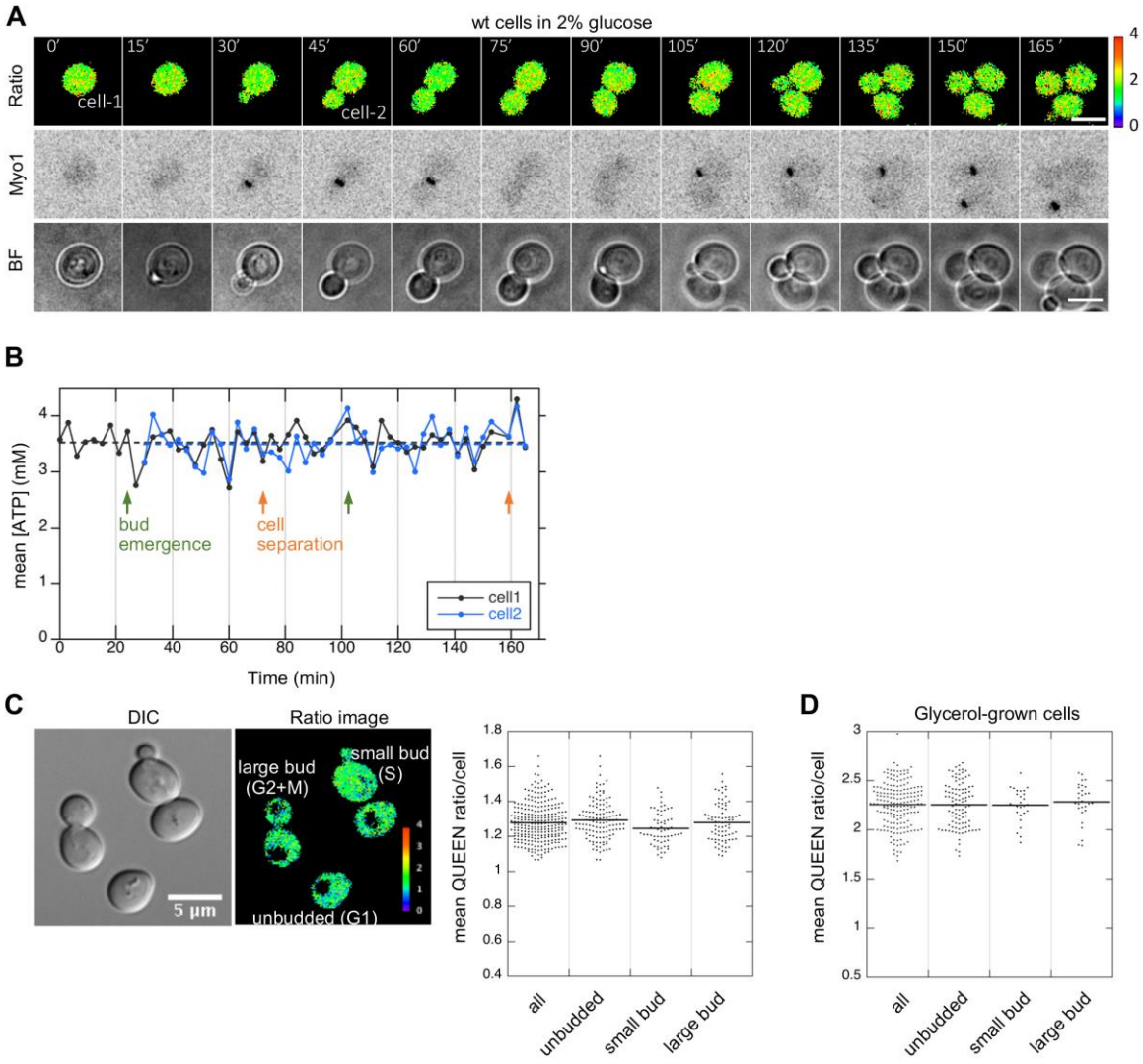

Fig. 3. Budding yeast ATP concentration is robustly maintained during mitotic cell cycle

(A and B) Long-term imaging of the QUEEN signal over generations. The images of the cells are shown in (A), and the ATP concentration translated from the QUEEN ratios of the two cells are plotted in (B). Dotted lines show the mean ATP concentration. Cell cycle events, such as bud emergence and cell separation as judged by the Myo1-mCherry signals are indicated by arrows. See also Movie S1. (C) Quantification of the QUEEN ratios at different budding stages growing in glucose. MTY3255 was grown to mid-log phase in SC + 2% glucose, and the QUEEN signals were imaged. Cells were classified according to their budding pattern, and the QUEEN ratio of each cell types was plotted. N = 61–125 cells were scored. DIC, differential interference contrast image. (D) Quantification of the QUEEN ratios at different budding stages growing in glycerol. MTY3255 was grown to mid-log phase in SC + 3% glycerol + 0.1% glucose, and the QUEEN signals were imaged. Cells were classified

according to their budding pattern, and the QUEEN ratio of each cell types was plotted. N = 27–56 cells. White scale bar = 5 μm.

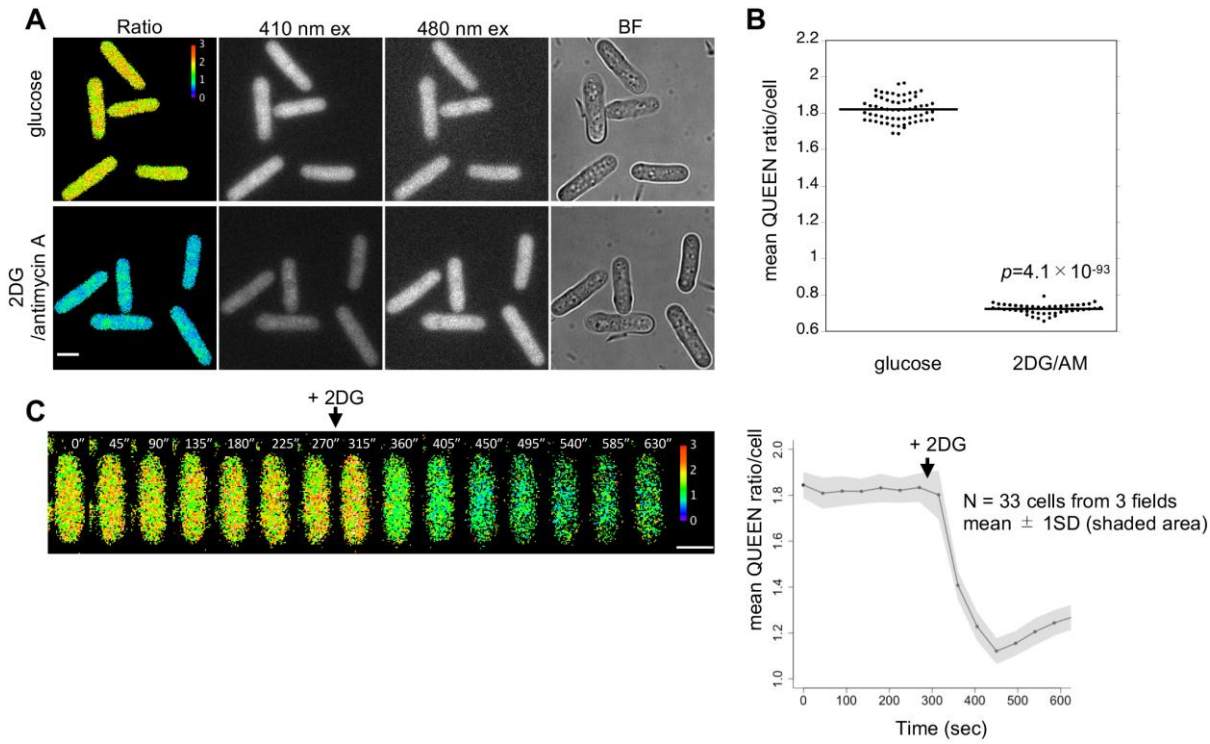

Fig. 4. QUEEN is a reliable ATP biosensor in the fission yeast

(A) Fluorescence images of the fission yeast cells expressing QUEEN. KSP3769 cells were grown in a medium containing 2% glucose and imaged before and after exposure to 20 mM 2DG and 10 µg/ml Antimycin A for 5min. (B) Dot plot of mean QUEEN ratio of cells shown in (A). N = 61 (glucose) and 46 (2DG/AM) cells were scored. (C) Rapid reduction in QUEEN ratio in cells treated with glycolytic inhibitor. The QUEEN ratio in KSP3769 cells grown in the 2% glucose was sequentially monitored, and the cells were supplemented with 2DG just after t = 270 s (indicated by an arrow) to give a final concentration of 22 mM glucose and 96 mM 2DG. The representative time-lapse image was shown (top). The QUEEN ratio at each time point was plotted (bottom). Data are the mean ± SD (shaded area), and collected from three fields of view. White scale bar = 5 µm.

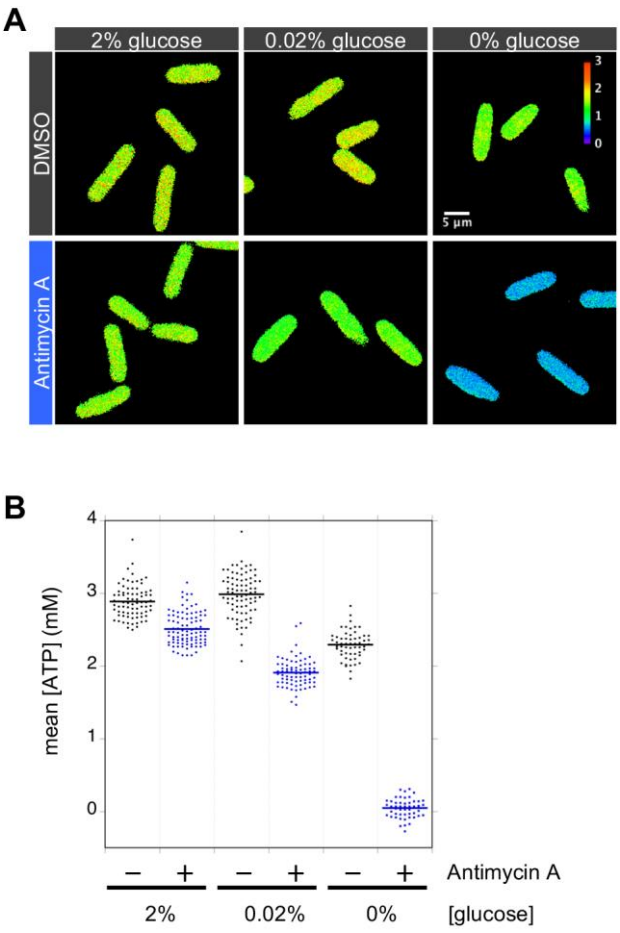

Fig. 5. Contribution of glycolysis and respiration on fission yeast ATP

(A) KSP3769 cells were grown in the 2% glucose, and then cultured in the medium containing 0%, 0.02%, or 2% glucose for six hours at 30°C. Cells were imaged before and after exposure to 10 µg/ml Antimycin A for 10 min. Representative images are shown. (B) The QUEEN ratios of the cells were translated into ATP concentration and are plotted. N = 50–93 cells were scored. White scale bar = 5 µm.

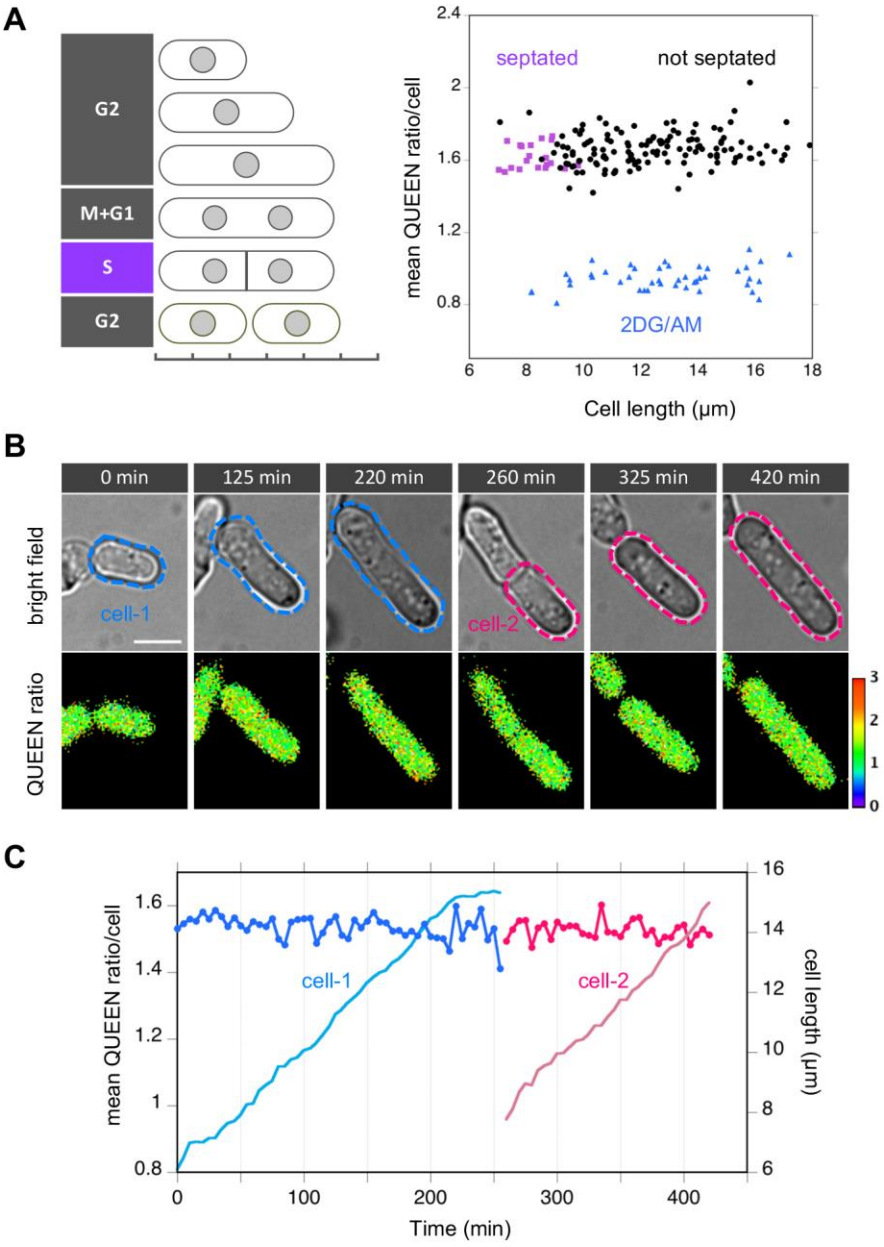

Fig. 6. ATP concentration in fission yeast cells remains constant during mitotic cell cycle and cell growth

(A) *Left*: Approximate relationship between cell cycle stages and cell length in fission yeast. Most of septated cells are in S-phase. *Right*: The QUEEN ratios of KSP3769 cells grown in the 2% glucose are plotted against cell length. Data labeled "2DG/AM" were from cells treated with 20 mM 2DG and 10 μg/ml antimycin A for 10 min. N = 20–135 cells were scored. (B) Long-term imaging of the QUEEN ratio in proliferating fission yeast cells. KSP3769 cells grown in the 2% glucose were imaged every 5 minutes for 12 h. (C) The QUEEN ratio (line with plots) and cell length (smooth line) of cells shown in (B) were plotted over time. White scale bar = 5 μm. See also Movie S2.

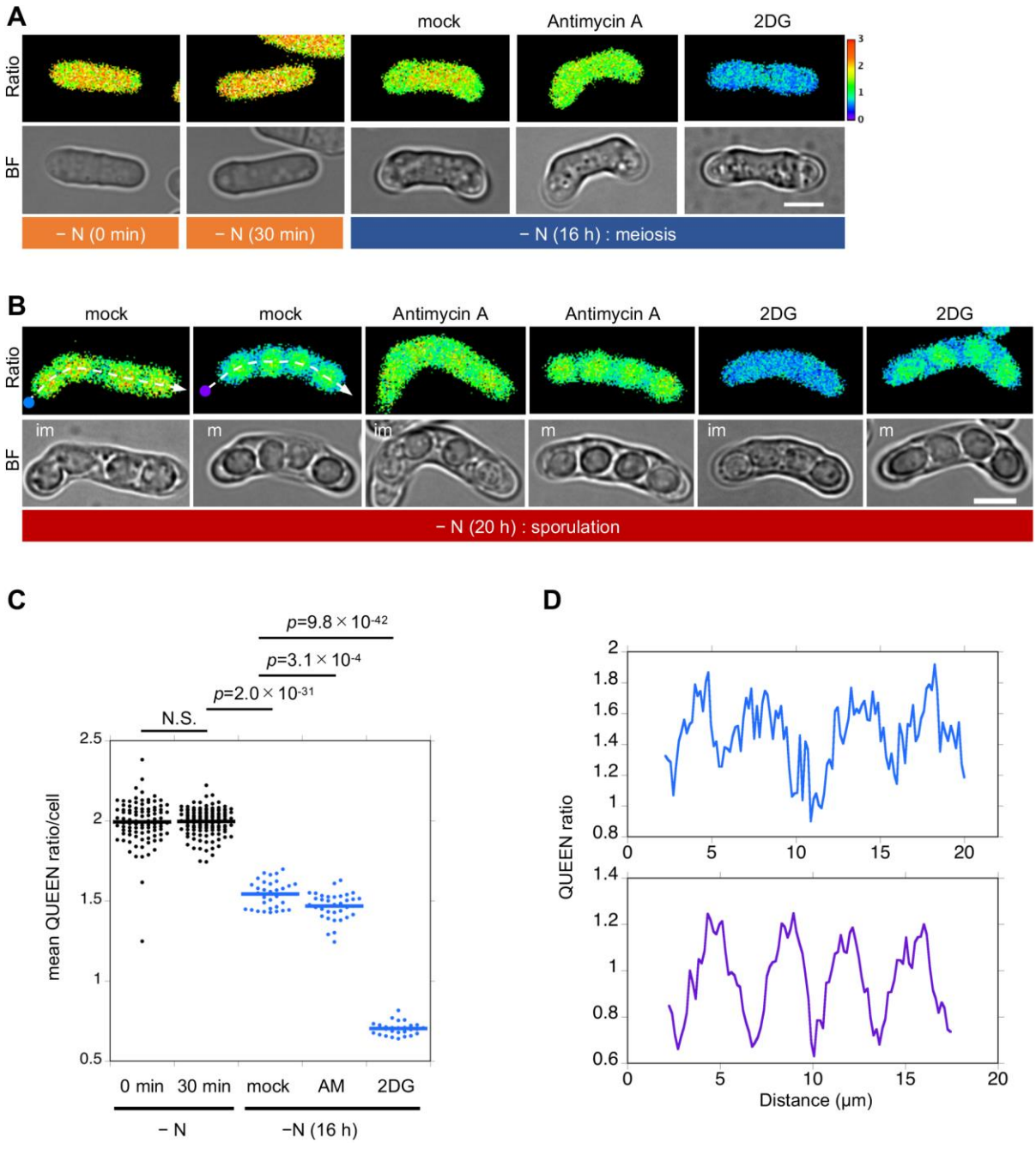

Fig. 7. ATP concentration is spatially and temporally regulated during meiosis and sporulation

(A) ATP level in fission yeast cells decreases during meiosis. MTY1162 cells were suspended in medium lacking nitrogen for 30 min or 16 hrs, and the QUEEN ratio was imaged. The QUEEN ratio was also imaged in the samples after 16hr-starvation of nitrogen were treated with 10 μg/ml antimycin A for 30 min or to 20 mM 2DG for 10 min. (B) Heterogeneity of ATP concentration in sporulating fission yeast cells. Sporulating MTY1162 cells were suspended in EMM−N medium and imaged. The samples were also treated with 10 μg/ml antimycin A or to 20 mM 2DG for 2 h. Ascus with immature spores (indicated by lower

contrast of their contours in BF image) or with mature spores is indicated by *im* or *m*, respectively. (C) Quantification of the data shown in (A). The QUEEN ratios of cells under the indicated conditions were plotted. N = 28–118 cells were scored. *P*-values indicating statistical significance are shown. (D) Local concentration of ATP in the spores. Line profiles of the QUEEN ratio along the cell length in sporulating cells indicated by dotted lines in (B). White scale bar = 5 μm.

Takaine et al. Fig. S1

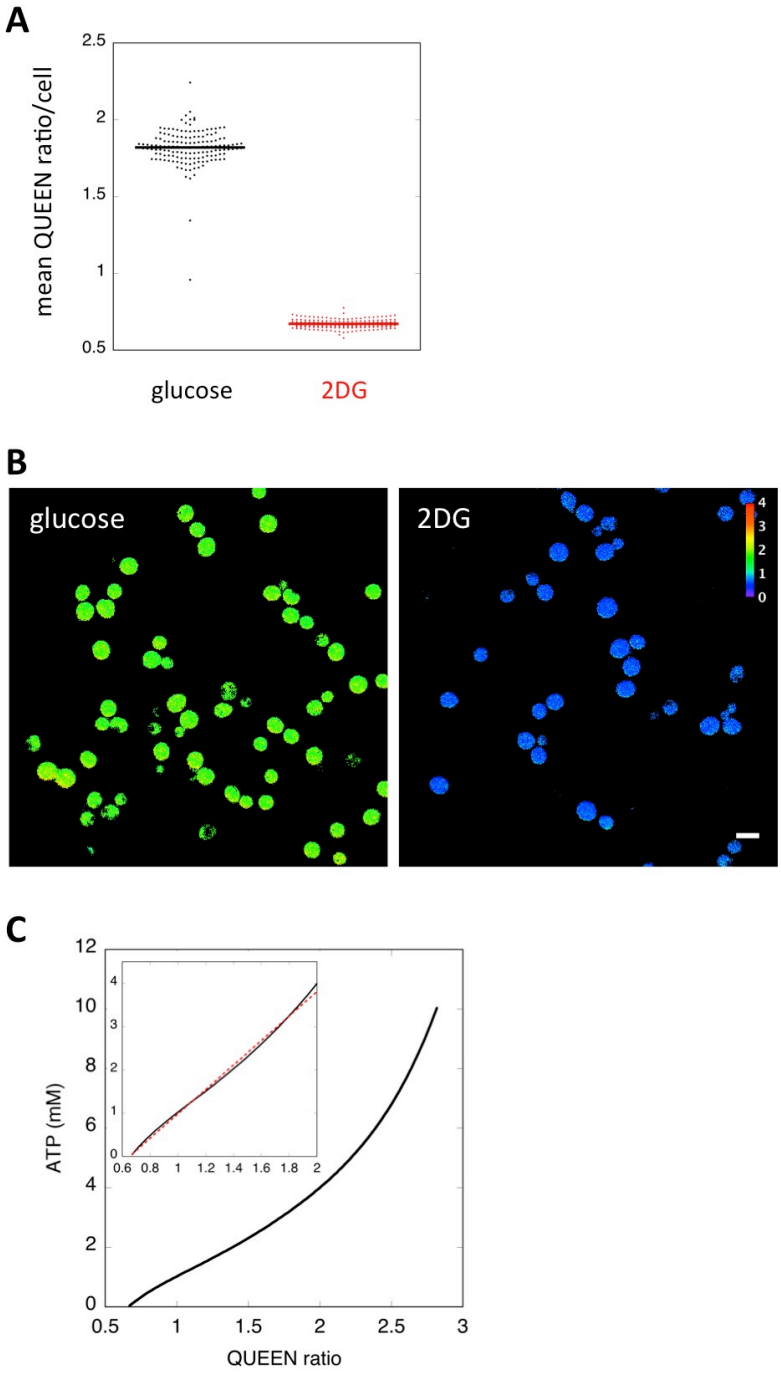

Fig. S1. Estimation of intracellular ATP level from the QUEEN ratio

(A) QUEEN ratios in cells after ATP depletion. MTY3264 cells were grown in SC + 2% glucose and imaged, or subjected to SC + 2% 2-deoxy-D-glucose (2DG) for 3 min and then imaged. The mean QUEEN ratio of each cell was dot plotted. N = 152 (glucose) and 175 (2DG) cells were scored. Assuming that the ATP is totally depleted after the treatment with 2DG, the QUEEN ratio of 0.671 equals 0 mM ATP in this experimental condition. (B)

Representative images of cells analyzed in (A). White scale bar = 5 μm. (C) A calibration curve of QUEEN-2m used for translation of QUEEN ratio to ATP concentration. The calibration curve previously published (Yaginuma et al., 2014) was represented by polynomial regression. Inset shows the curve in the QUEEN ratio range from 0.6 to 2.0, and a dotted line indicates a linear regression. Note that ATP level is almost proportional to the QUEEN ratio in this range.

Takaine et al. Fig. S2

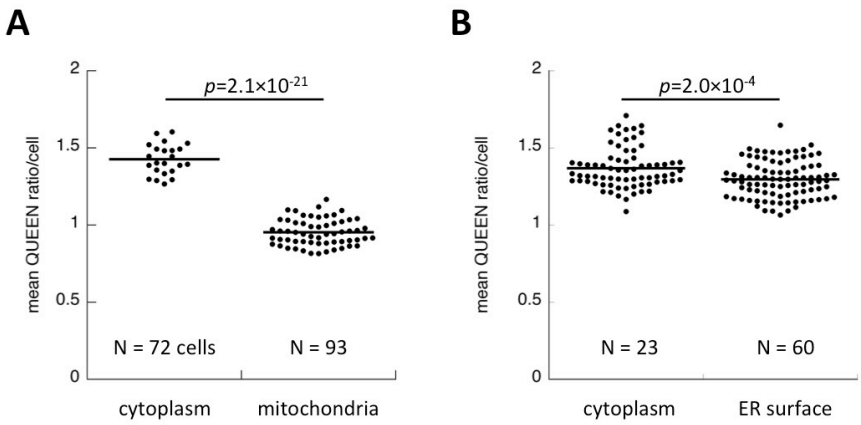

Fig. S2. QUEEN ratio in mitochondrial matrix and on the surface of ER

Quantification of the data shown in Fig. 1F. The mean ratios of mitQUEEN (A) and erQUEEN (B) in individual cells were plotted. The mean ratios of cytoplasmic QUEEN were also plotted for comparison**.**

Table S1. *Budding yeast strains used in this study*

Name	Genotype	Source	Fig.
MTY3015	*his3Δ1 leu2Δ0 lys2Δ0 ura3Δ0*	Lab stock	(parental strain of MTY3255 and MTY3261)
MTY3255	*his3Δ1::2×pRS303-P_{TEF}-QUEEN-2m-T_{CYC1} leu2Δ0 lys2Δ0 ura3Δ0*	This study	1B, 1C, 2, 3C, S2
MTY3261	*his3Δ1::3×pRS303-P_{TEF}-QUEEN-2m-T_{CYC1} leu2Δ0 lys2Δ0 ura3Δ0*	This study	(parental strain of MTY3264)
MTY3153	*his3Δ1::2×pRS303-P_{TEF}-QUEEN-2m-T_{CYC1} leu2Δ0 lys2Δ0 ura3Δ0 gph1Δ::kanMX6*	This study	1D
MTY3226	*his3Δ1::pRS303-Ptef1-mito-QUEEN-2m leu2Δ0 lys2Δ0 ura3Δ0*	This study	1F, S2
MTY3229	*his3Δ1::2×pRS303-Ptef1-SEC71TMD-QUEEN-2m leu2Δ0 lys2Δ0 ura3Δ0*	This study	1F, S2
MTY3264	*his3Δ1::3×pRS303-P_{TEF}-QUEEN-2m-T_{CYC1} leu2Δ0 lys2Δ0 ura3Δ0 MYO1-3mCherry-hphMX6*	This study	1E, 3A-B, S1

Table S2. *Fission yeast strains used in this study*

Name	Genotype	Source	Fig.
KSP3769	*leu1-32::Ptif51-QUEEN2m::leu1*$^{+}$ *h*$^{-}$	Ito et al., 2019 (accepted)	4, 5, 6
MTY1162	*leu1-32::Ptif51-QUEEN2m::leu1*$^{+}$ *h*^{90}	This study	7

Table S3. *Plasmids used in this study*

Name	Structure	Source	Purpose
MTP0017	pFA6a-3mCherry-hphMX6	Lab stock	MTY3264
MTP3001	pRSET-QUEEN-2m	Lab stock; Yaginuma et al., 2014	MTP3051
MTP3007	pSP-G2	Partow et al., 2010; YGRC	MTP3051
MTP3051	pSP-G2-QUEEN-2m	This study	MTP3067
MTP3067	pRS303-P_{TEF}-QUEEN-2m-T_{CYC1}	This study	MTY3255, 3261

Supplementary movies

Movie1

Long-term imaging of QUEEN in budding yeast cells over several generations. Corresponding to the data shown in Fig. 3A. Left, the QUEEN ratio image; middle, Myo1-mCherry (inverted grayscale image); right, bright field image. MTY3264 cell was grown in SC + 2% glucose and imaged every 3 minutes. White scale bar = 5 µm.

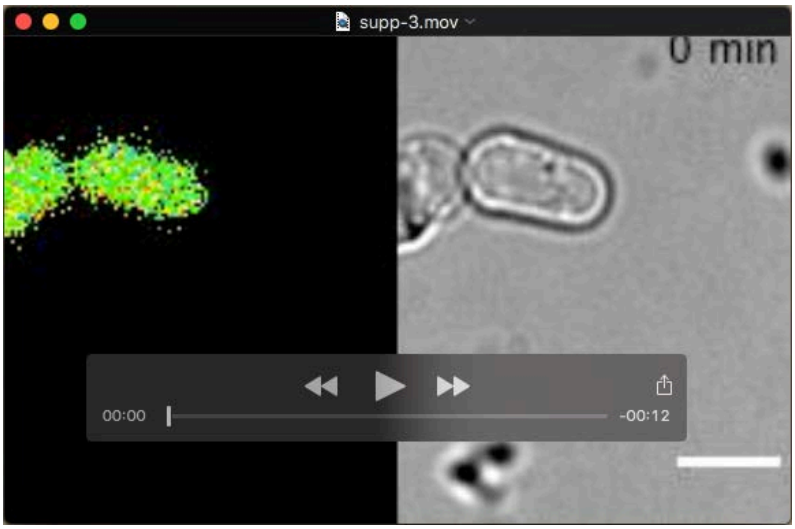

Movie 2

Long-term imaging of QUEEN in fission cells. Corresponding to the data shown in Fig. 6B. Left, the QUEEN ratio image; right, bright field image. KSP3769 cell was grown in EMM (containing 2% glucose) and imaged every 5 minutes. White scale bar = 5 µm.